UCRL-JC-130147
PREPRINT

Linear X-Ray Line Polarization Effects on Spectral Measurements Using an Electron Beam Ion Trap

Peter Beiersdorfer

This paper was prepared for submittal to the
Proceedings of the US - Japan Workshop on Plasma Polarization on Spectroscopy
Kyoto, Japan
January 26-28, 1998

March 5, 1998

Lawrence Livermore National Laboratory

This is a preprint of a paper intended for publication in a journal or proceedings. Since changes may be made before publication, this preprint is made available with the understanding that it will not be cited or reproduced without the permission of the author.

DISCLAIMER

This document was prepared as an account of work sponsored by an agency of the United States Government. Neither the United States Government nor the University of California nor any of their employees, makes any warranty, express or implied, or assumes any legal liability or responsibility for the accuracy, completeness, or usefulness of any information, apparatus, product, or process disclosed, or represents that its use would not infringe privately owned rights. Reference herein to any specific commercial product, process, or service by trade name, trademark, manufacturer, or otherwise, does not necessarily constitute or imply its endorsement, recommendation, or favoring by the United States Government or the University of California. The views and opinions of authors expressed herein do not necessarily state or reflect those of the United States Government or the University of California, and shall not be used for advertising or product endorsement purposes.

Linear X-Ray Line Polarization Effects on Spectral Measurements Using an Electron Beam Ion Trap

Peter Beiersdorfer

Department of Physics and Space Technology
Lawrence Livermore National Laboratory, Livermore, CA 94550, USA

Line emission from an electron beam ion trap (EBIT) source is produced in the collision of trapped ions with a uni-directional electron beam and generally is linearly polarized. This polarization must be taken into account when using spectrocopic data to infer cross sections for electron-ion interaction processes. A good theoretical and experimental understanding of polarization effects is, therefore, paramount for accurate measurements. On the other hand, the source provides a unique environment for measuring the amount of linear polarization under very well controlled conditions. As a result, predictions of linear polarization caused by uni-directional electron impact can be tested. A review of polarization effects on spectral measurements employing an EBIT source is given. The technique for measurements of the linear line polarization using the two crystal technique is discussed, and new results for the polarized K-shell emission from heliumlike Fe^{24+} for energies up to 120 keV are presented.

1. Introduction

The Electron Beam Ion Trap (EBIT) device utilizes a dense ($< 5 \times 10^{12}$ cm^{-3}) mono-energetic beam of electrons to produce and excite highly charged ions from virtually any element or isotope of choice. By analyzing the line radiation emitted in the interaction between the ions and the electron beam, cross sections can be determined for the particular electron-ion interaction process studied. For example, the device has been used to measure the electron-impact excitation cross sections of the K-shell transitions in heliumlike Ti^{20+} through Fe^{24+} [1,2], the resonance strengths of dielectronic recombination satellites [3], including those involving high-n spectator satellites [4,5], and the cross sections for electron-impact ionization of lithiumlike ions [6]. The device has also been used to measure indirect excitation processes such as innershell ionization and radiative cascades [7].

As was shown in Refs. [8] and [9], quasi-stationary ions colliding with unidirectional electrons emit line radiation that is generally both anisotropic and polarized. Therefore, the intensity of a specific line depends on the observation angle relative to the axis defined by the electron beam and on whether or not the emission is analyzed with a polarization-sensitive instrument. Polarization phenomena, thus, play an important role in EBIT measurements, and, if not taken properly into account, can lead to results that are wrong. This means that cross section measurements on an EBIT, even measurements of relative cross sections, require a good understanding of polarization effects.

While polarization effects complicate the analysis of spectral line formation processes in EBIT, these effects can be measured directly and the amount of linear polarization can be inferred. In fact, EBIT represents a unique spectroscopic facility for studying alignment processes in highly charged ions by directional electrons in a

controlled, well characterized laboratory environment.

Here, we review the measurements of linear polarization of x-ray lines that have been performed with the EBIT source, and we present the results of recent measurements that show that the EBIT technique can be used to measure the linear polarization not only at threshold, but also at energies ten to twenty times the threshold energy, or, in the case of the Fe^{24+} K-shell lines at electron energies above 100 keV. Such high-energy measurements are of special importance for polarization spectroscopy. In many plasmas, polarized line emisstion is produced by a suprathermal tail in the electron distribution function with energies that are orders of magnitude larger than the bulk thermal energy. The testing of theoretical predictions of ion alignment away from the threshold energy for line excitation is therefore of critical importance for evaluating the predictive capabilities of theory.

2. Anisotropy of the Emitted Radiation

For the conditions given in an EBIT, we assume quasi-stationary ions colliding with electrons traveling along the z-direction, i.e., we assume cylindrical symmetry. This is a good assumption as long as the electron beam energy is large compared to the thermal energy of the electrons. (In the case where this assumption does not hold, see the contribution by Savin, Gu, and Beiersdorfer in these Proceedings). Using the formalism developed by Steffen and Alder [10], the two intensity components of linearly polarized line radiation with electric field vector parallel and perpendicular to the electron beam direction can then be described by

$$I_{\|}(\vartheta) = \frac{1}{8\pi} \sum_{\lambda=even} B_\lambda A_\lambda [P_\lambda(\vartheta) + \Gamma(\kappa) f_\lambda P_\lambda^2(\vartheta)] \langle I_{\|} \rangle \tag{1}$$

and

$$I_{\perp}(\vartheta) = \frac{1}{8\pi} \sum_{\lambda=even} B_{\lambda} A_{\lambda} [P_{\lambda}(\vartheta) - \Gamma(\kappa) f_{\lambda} P_{\lambda}^{2}(\vartheta)] \langle I_{\perp} \rangle, \tag{2}$$

as discussed in more detail in Ref. [11]. Here, B_{λ} is the orientation parameter; A_{λ} is the angular distribution coefficient; $P_{\lambda}(\vartheta)$ and $P_{\lambda}^{2}(\vartheta)$ represent the Legendre and associated Legendre polynominal, respectively; $\langle I_{\|} \rangle$ and $\langle I_{\perp} \rangle$ are the 4π-averaged intensity components. We assume that the emitted radiation is described by a single multipole operator where λ represents the multipole order of the emitted radiation.

The parameters B_{λ} are given by

$$B_{\lambda} = \sum_{m} (-1)^{J_i+m} [(2\lambda+1)(2J_i+1)]^{1/2} \begin{pmatrix} J_i & J_i & \lambda \\ -m & m & 0 \end{pmatrix} \sigma_m. \tag{3}$$

Here J_i is the initial total angular momentum, m is the magnetic quantum number, and σ_m is the population density of each respective sublevel normalized such that $\Sigma_m \sigma_m = 1$. The large parentheses denote the Wigner 3-j symbol. The angular distribution coefficient A_{λ} is given by

$$A_{\lambda} = (-1)^{J_i+J_f-1} [(2\lambda+1)(2J_i+1)]^{1/2} (2L+1) \begin{pmatrix} L & L & \lambda \\ 1 & -1 & 0 \end{pmatrix} \begin{Bmatrix} L & L & \lambda \\ J_i & J_i & J_f \end{Bmatrix} \tag{4}$$

L represents the order of pure 2^L multipole decays. The large braces denote the Wigner 6-j symbol. The coefficient f_{λ} is given by

$$f_{\lambda} = -\left[\frac{(\lambda-2)!}{(\lambda+2)!}\right]^{1/2} \frac{\begin{pmatrix} L & L & \lambda \\ 1 & 1 & -2 \end{pmatrix}}{\begin{pmatrix} L & L & \lambda \\ 1 & -1 & 0 \end{pmatrix}}. \tag{5}$$

The function $\Gamma(\kappa)$ determines the sign. For electric multipole transitions it equals $\Gamma(E) = 1$, for magnetic multipole transitions it equals $\Gamma(M) = -1$.

The intensity variation of the emitted radiation $I(\vartheta)$ is given by the sum of $I_{\|}(\vartheta)$ and $I_{\perp}(\vartheta)$:

$$I(\vartheta) = \frac{1}{4\pi} \sum_{\lambda=even} B_\lambda A_\lambda P_\lambda(\vartheta) \langle I_s \rangle. \tag{6}$$

Here, $\langle I_s \rangle$ is the 4π-averaged line source intensity, i.e.,

$$\int I(\vartheta) d\Omega = \langle I_s \rangle. \tag{7}$$

Defining the linear polarization P at an observation angle $\vartheta = 90^o$ relative to the z-axis as the fractional difference between the intensity of light with electric field vector parallel to the beam direction, $I_{\|}$, and the intensity of light with electric field vector perpendicular, $I_{\perp}$,

$$P = \frac{I_{\|}(90^o) - I_{\perp}(90^o)}{I_{\|}(90^o) + I_{\perp}(90^o)}, \tag{8}$$

and evaluating the coefficients in Eq. (6), we find the following expressions for the angular variation of the intensity of the emitted light. For an electric dipole (E1) transitions (with $L = 1$) we find

$$I(\vartheta) = \frac{3}{4\pi} \frac{1 - P\cos^2\vartheta}{3 - P} \langle I_s \rangle. \tag{9}$$

For a magnetic dipole (M1) transitions ($L = 1$) we find

$$I(\vartheta) = \frac{3}{4\pi} \frac{1 + P\cos^2\vartheta}{3 + P} \langle I_s \rangle. \tag{10}$$

Generally, the angular intensity variation of higher-order multipole transitions cannot be expressed as a simple expression of P. In the case of the $1s2p\ ^3P_2 \rightarrow 1s^2\ ^1S_0$ magnetic dipole quadrupole (M2) transition ($L = 2$) in heliumlike systems, one can show that $B_4(^3P_2) << B_2(^3P_2)$. For the case of heliumlike Fe^{24+} it was shown in Ref. [11] that $B_4(^3P_2)/B_2(^3P_2) \approx 1.6 \times 10^{-3}$. Thus, this M2 transition behaves as a dipole transition. In particular, its angular intensity variation is given by

$$I(\vartheta) = \frac{3}{4\pi} \frac{1 - P\cos^2\vartheta}{3 - P} \langle I_s \rangle, \tag{11}$$

i.e., it is identical to that of E1 transitions.

The anisotropy in the line emission of linearly polarized lines can be illustrated by looking at the spectra predicted for the K-shell emission of heliumlike Fe^{24+}. At threshold of excitation and ignoring cascade effects, the polarizations of the four K-shell transitions in Fe^{24+} have been predicted in Refs. [12] to be +0.584, −0.518, −0.196, and 0.0 for the transitions $1s2p\ ^1P_1 \rightarrow 1s^2\ ^1S_0$ (labeled w in the notation of Ref. [14]), $1s2p\ ^3P_2 \rightarrow 1s^2\ ^1S_0$ (labeled x), $1s2p\ ^3P_1 \rightarrow 1s^2\ ^1S_0$ (labeled y), and $1s2s\ ^3S_1 \rightarrow 1s^2\ ^1S_0$ (labeled z), respectively. A comparison of the 4π-average spectral emission with that observed at $\vartheta = 0^o$ and $\vartheta = 90^o$ is given in Fig. 1. Because the angular dependence of the emission is different for each line, there are dramatic differences in the spectral shape when looking at different observation angles relative to the electron beam direction. In fact, the ratio of the intensities of w and x changes by a factor of about three when the viewing angle is changed from $\vartheta = 0^o$ to $\vartheta = 90^o$.

A second example of the angular dpendence of the emitted line radiation is given in Fig. 2, where we show the predicted spectra of the K-shell satellites of Fe^{24+} produced by the KLL dielectronic recombination resonances. These lines are all electric dipole transitions. Their polarizations have been given by Inal and Dubau [13], ranging from −0.75 to +0.60. Again, a dramatic difference can be seen when comparing the spectral emission at $\vartheta = 0^o$ with that at $\vartheta = 90^o$, or with the 4π averaged emission. From these examples it is very clear that it is imperative that the polarization of every line is known lest significant uncertainties in the line intensities are made.

The construction of the EBIT allows viewing of the ions in the trap via radial ports, i.e., in the plane perpendicular to the electron beam direction at $\vartheta = 90^o$, as shown in Fig. 3. A direct view into the trap along the axis of the electron beam at $\vartheta = 90^o$ is possible as well. The solid angle subtended by the latter line of sight is, however, very small because any axial spectrometer must be placed about 10 times

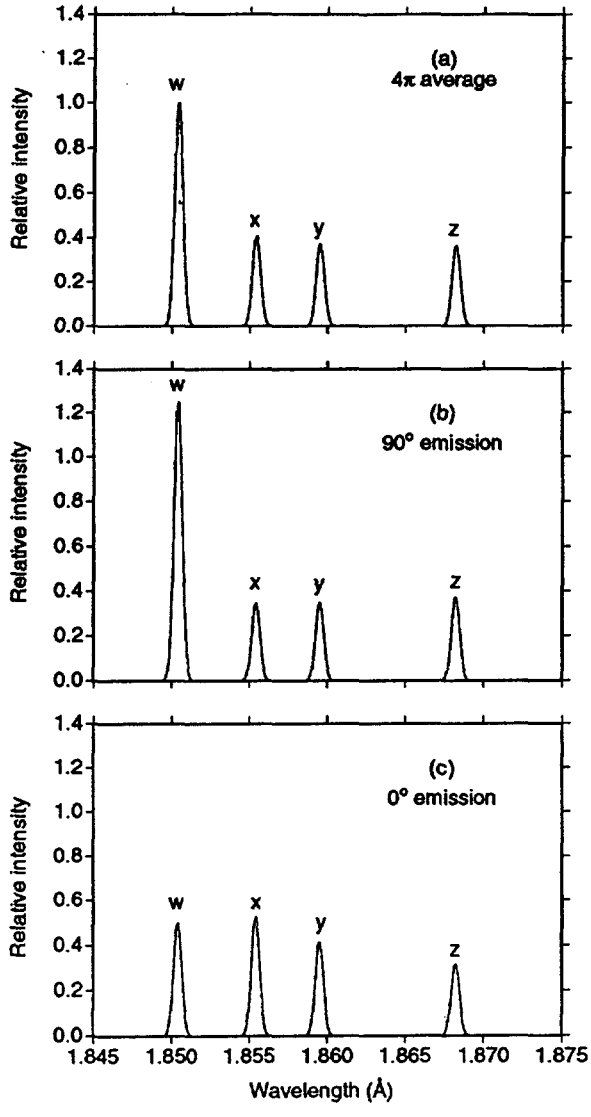

Figure 1: Predicted spectral line intensities of the resonance line w, the intercombination lines x and y, and the forbidden line z in heliumlike Fe^{24+} excited by collisions with a 6850-eV electron beam: (a) emission averaged over a 4π solid angle; (b) emission observed at an angle $\vartheta = 90^o$, i.e., in the plane perpendicular to the electron beam direction; (c) emission observed at an angle $\vartheta = 0°$, i.e., a line of sight along the electron beam direction.

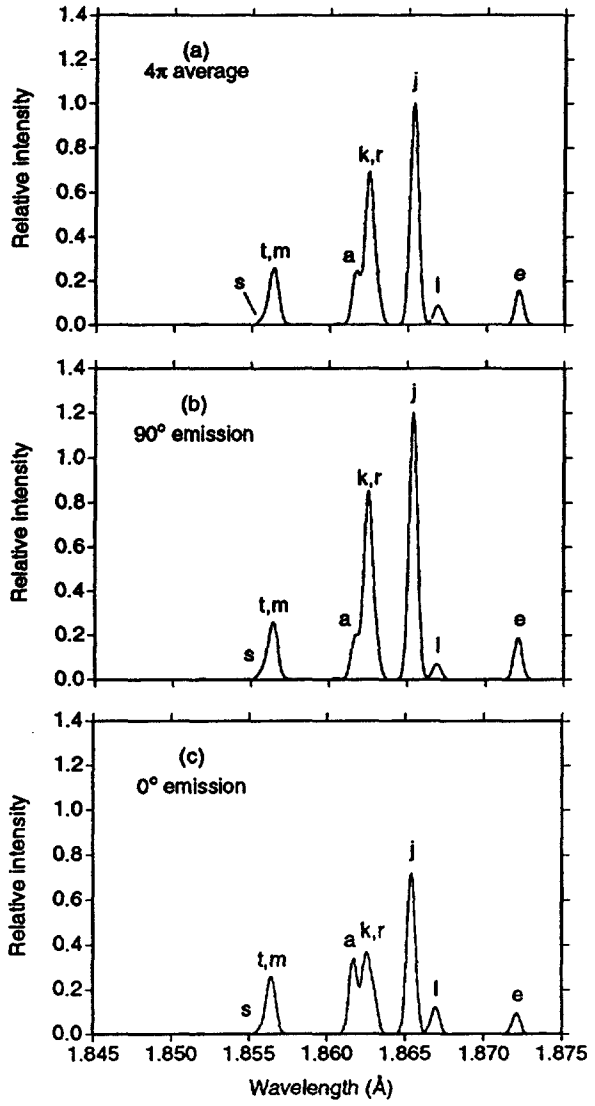

Figure 2: Predicted spectral line intensities of the $2 \rightarrow 1$ dielectronic satellite transitions of heliumlike Fe^{24+} produced by KLL resonant electron capture: (a) emission averaged over a 4π solid angle; (b) emission observed at an angle $\vartheta = 90^o$, i.e., in the plane perpendicular to the electron beam direction; (c) emission observed at an angle $\vartheta = 0^o$, i.e., a line of sight along the electron beam direction. The transitions are labeled in standard notation (cf. Ref. [14]).

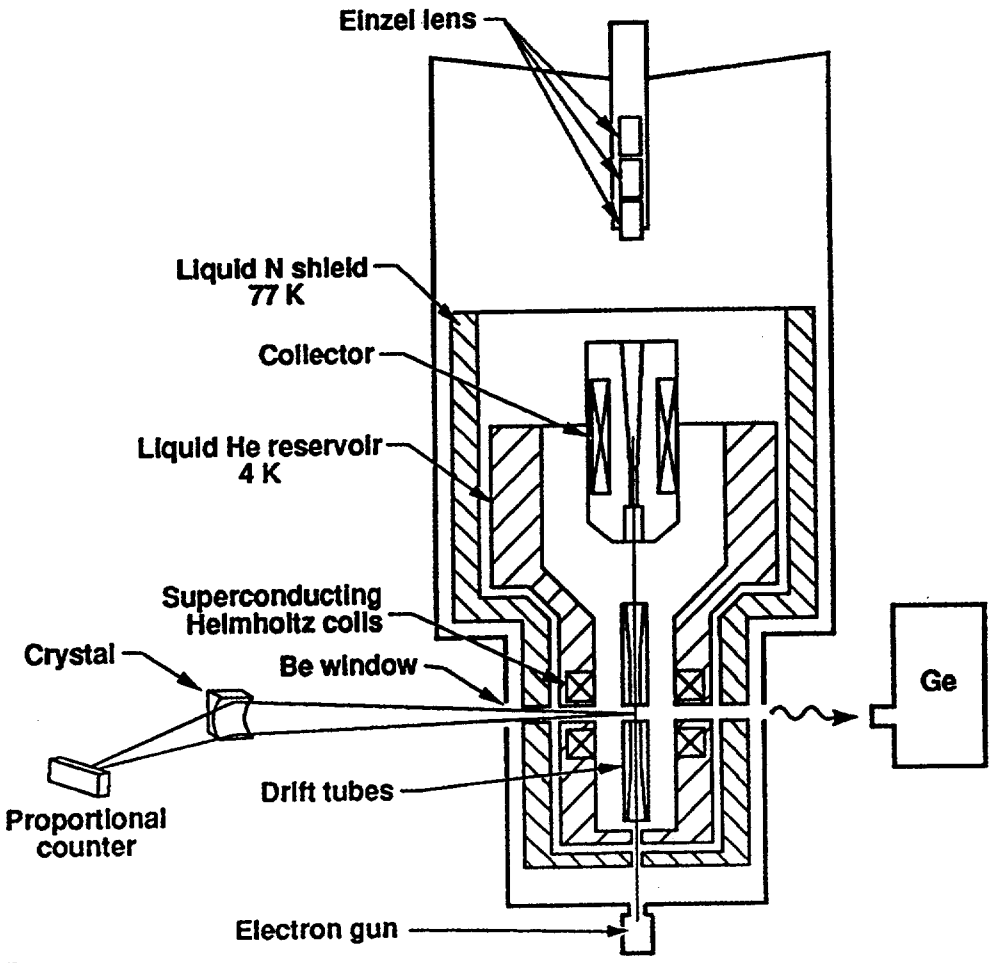

Figure 3: Schematic layout of the crystal-spectrometer on the LLNL EBIT facility. Ions are produced and trapped in a 2-cm long region between the superconducting Helmholtz coils. The ions are excited by an electron beam propagating between the electron gun and the collector. X rays are analyzed and dispersed with crystal spectrometers in the plane perpendicular to the direction of the electron beam.

further away from the trap than any radial spectrometer. As result, all line emission spectra from highly charged ions have so far been recorded at observation angles of $\vartheta = 90^o$.

3. Crystal-Spectrometer Measurements

The use of crystal spectrometers adds another dimension to the complexity of accurate interpretation of polarized x-ray line emission. The reflectivity of a given crystal depends on whether the electric field vector lies parallel or perpendicular to the diffraction plane. Moreover, the reflectivity for each polarization component depends on the Bragg angle and the type of crystal (for some crystal types on the individual specimen) used. The relative intensities of the observed spectral lines will thus depend on the type of crystal, the Bragg angle, and value of the linear polarization of each line.

The intensity of an x-ray line observed on EBIT with a crystal spectrometer at 90° to the beam direction can be written as

$$I^{obs} = R_{||} I_{||} + R_{\perp} I_{\perp}. \tag{12}$$

Here, $R_{||}$ and $R_{\perp}$ are the integrated crystal reflectivities for x rays polarized parallel and perpendicular to the electron beam directions, i.e., perpendicular and parallel to the plane of dispersion, respectively.

The ratio $R = R_{\perp}/R_{||}$ depends strongly on the Bragg angle θ, as illustrated in Fig. 4. For mosaic crystals the ratio varies as $\cos^2(2\theta)$; for perfect crystals it varies as $|\cos(2\theta)|$ [15]. The ratio for actual crystals lies in between the two extremes. Most crystals approach the values for perfect crystals although the value of R is typically reduced by absorption. Calculations of integrated reflectivities of perfect crystals can be found, for example, in Ref. [16].

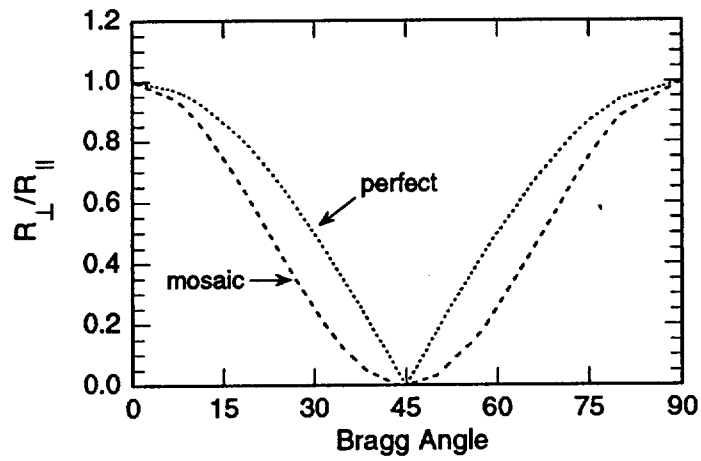

Figure 4: Variation of the relative crystal reflectivities $R_\perp/R_{||}$ for x rays polarized perpendicular and parallel to the electron beam direction. The dotted line represents the values for a mosaic crystal; the dashed line represents the values for an ideal crystal. At a Bragg angle of 45° the reflection of the perpendicular component vanishes for any type of crystal, $R_\perp/R_{||} = 0$.

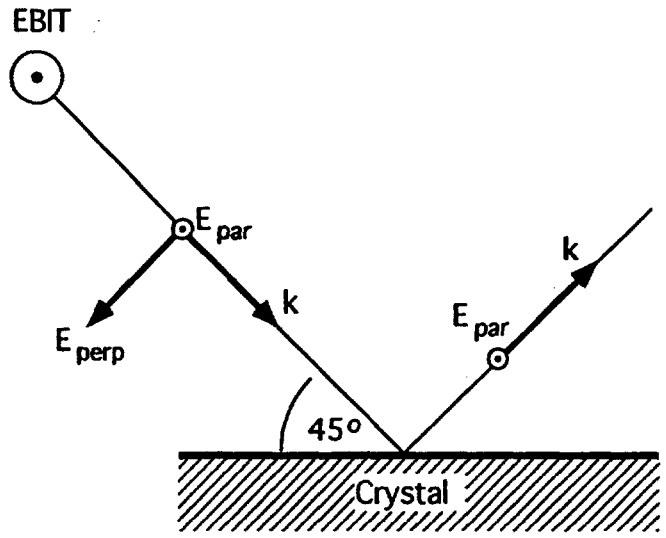

Figure 5: Schematic diagram of the reflection of linearly polarized x rays off a crystal surface at a Bragg angle of 45°. The electron beam is in the direction out of the page as indicated at the EBIT position. The plane of dispersion of the crystal is perpendicular to the beam direction. Only the parallel polarization state is reflected; the polarization state perpendicular to is completely absorbed by the crystal.

Because analyzing crystals reflect the two polarization components differently the intensity observed with crystal spectrometers differs from the emitted intensity. The effect is strongest at $\theta = 45^o$ where $I_\perp$ vanishes and only $I_\parallel$ is observed, as illustrated in Fig. 5. Consequently, the intensity of negatively polarized lines, i.e., lines with $I_\perp > I_\parallel$ are disproportionally reduced when observed near $\theta = 45^o$. Positively polarized lines appear enhanced. Near $\theta = 90^o$ or 0°, both polarization components are reflected nearly equally, and the observed spectra are the least altered by crystal effects.

For the spectrum of heliumlike iron, the polarization depedendence of the crystal

reflectivity means that line w will be enhanced, while lines y and especially x are strongly reduced when observed near $\theta = 45^o$. This was indeed observed and reported in Ref. [17]. The two spectra of Fe^{24+} simultaneously observed with two different crystals in Ref. [17] are shown in Fig. 6. The first spectrometer used a LiF(220) crystal with lattice spacing $2d = 2.848$ Å and observed the lines at a nominal Bragg angle of 41°. The second used a Si(220) crystal with lattice spacing $d = 3.840$ Å and observed the lines at a nominal Bragg angle of 29°. The relative reflectivities $R_\perp/R_\parallel = 0.48$ for Si(220) and $R_\perp/R_\parallel = 0.12$ for LiF(220) [16]. As expected from the difference in the relative crystal reflectivities, the relative intensities of the four heliumlike lines differ notably in the two spectra. The triplet lines are suppressed relative to the singlet line intensity in both spectra, but this suppression is much more pronounced in the spectrum obtained with the LiF(220) crystal. Predictions of the spectral line emission based on the values of the relative reflectivities are also shown in Fig. 6, and good agreement with the measurements is found. Again, it is clear from this discussion that it is imperative that the amount of linear polarization is known. Moreover, it is very important to account for the crystal spectrometer response to the polarized line emission.

4. Measurements of the Degree of Linear X-ray Line Polarization

While the dependence of the observed spectral line emission on the amount of polarization, the Bragg angle, and the type of crystal employed in the observation complicates the analysis of spectral data from an EBIT device, it also represents a unique opportunity. By making simultaneous measurements of x-ray line spectra with two spectrometers, such as those presented in Fig. 6, the degree of linear polarization

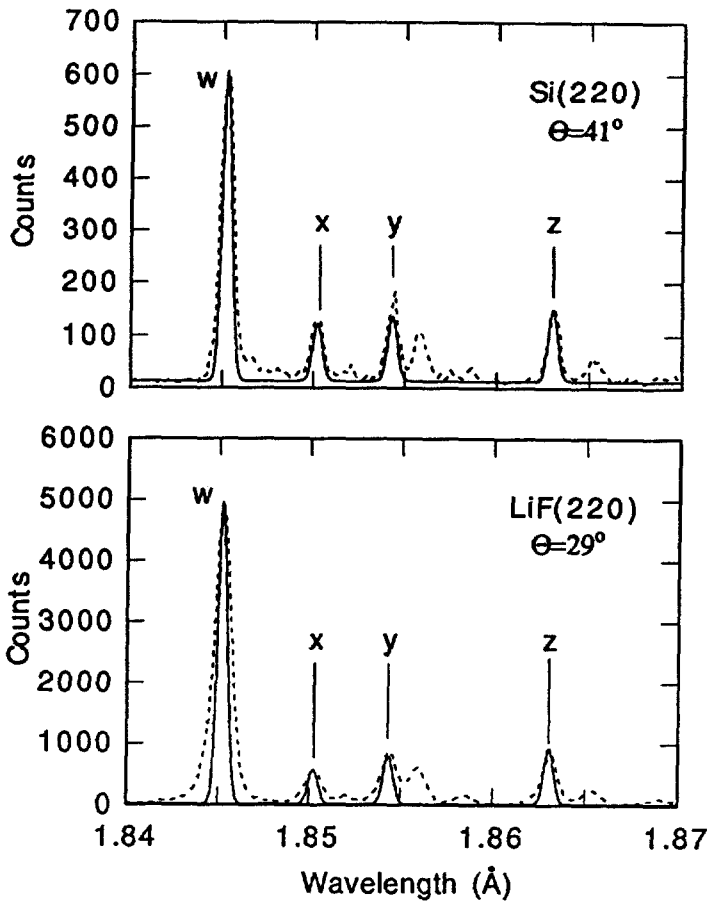

Figure 6: Crystal-spectrometer spectra of the four lines w, x, y, and z in heliumlike Fe^{24+} excited by direct electron-impact excitation by a 6850-eV electron beam (dashed lines). The top spectrum was obtained with a Si(220) crystal at a Bragg angle of about 41°; the bottow spectrum was obtained with a LiF(220) crystal at a Bragg angle of about 29°. Unlabled features are from lower charge states of iron. The predicted spectral intensities (solid lines), normalized to the intensity of line w, are superimposed for comparison.

of a given line can be determined provided the relative crystal reflectivities are known and the two spectra can be normalized to each other with the help of lines that have a known amount of linear polarization.

Making use of Eq. (12), the intensity ratio of two lines a and b observed with crystal $C1$ is given by

$$\frac{I^a}{I^b}|_{C1} = \frac{I^a_{\parallel} + R_{C1} I^a_{\perp}}{I^b_{\parallel} + R_{C1} I^b_{\perp}}. \tag{13}$$

Here, we assumed that $R = R_{\perp}/R_{\parallel}$ is constant in the range of Bragg angles spanned by the two lines. Similarly, the ratio of the two lines observed with crystal $C2$ is

$$\frac{I^a}{I^b}|_{C2} = \frac{I^a_{\parallel} + R_{C2} I^a_{\perp}}{I^b_{\parallel} + R_{C2} I^b_{\perp}}. \tag{14}$$

Making use of Eq. (8) and combing Eqs. 13 and 14, we can express the polarization P_a of line a in terms of the polarization P_b of line b:

$$P_a = \frac{\frac{I^a}{I^b}|_1(1 + R_1\frac{1-P_b}{1+P_b})(R_2+1) - \frac{I^a}{I^b}|_2(1 + R_2\frac{1-P_b}{1+P_b})(R_1+1)}{\frac{I^a}{I^b}|_1(1 + R_1\frac{1-P_b}{1+P_b})(R_2-1) - \frac{I^a}{I^b}|_2(1 + R_2\frac{1-P_b}{1+P_b})(R_1-1)} \tag{15}$$

From Eq. (15) it follows that the polarization of a given line can be determined by measuring the difference of its intensity when looked at with two spectrometers relative to that of the known line.

Because transitions from upper levels with total angular momentum J=1/2 are stricly unpolarized, they provide excellent reference lines for polarization measurements. This fact has been used by Savin *et al.*, as discussed in these proceedings. They measured the polarization of the $4p_{3/2} \rightarrow 2s_{1/2}$ transition in lithiumlike Fe^{23+} by comparing it to the close by and unpolarized $4p_{1/2} \rightarrow 2s_{1/2}$ transition.

In the following, we are concerned about the polarization of the heliumlike K-hell transitions. No unpolarized line exists among the heliumlike transitions. However, near threshold for electron-impact excitation the polarization of the forbidden line z is

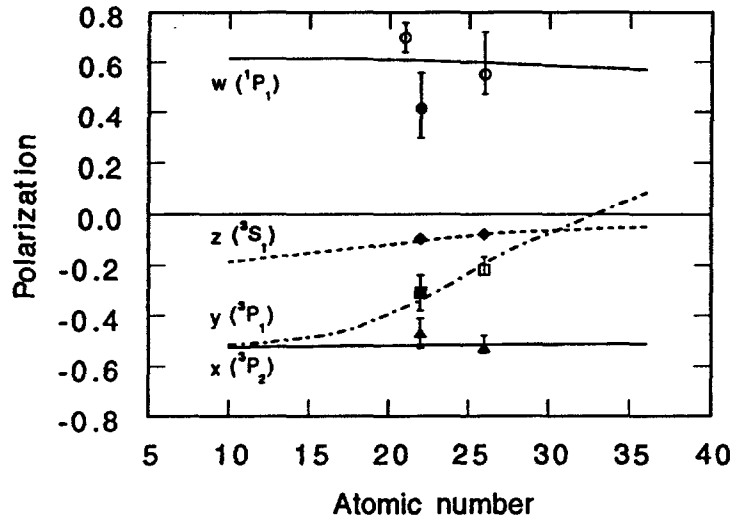

Figure 7: Predicted polarizations of the four $2 \rightarrow 1$ transitions w, x, y, and z in the heliumlike ions Ne^{8+} through Kr^{34+}. The predictions are for nuclei without a magnetic moment. The newly measured values for Ti^{20+} from Ref. [18] are shown for comparison. Also shown are the measured values for Fe^{24+} from Ref. [11] and the value for the resonance line in Sc^{19+} from Ref. [19].

completely determined by that of line x because of cascade contributions, as discussed in Ref. [11]. This linkage was shown to enable a determination of the polarization of all observed lines in the heliumlike K-shell spectrum in the absence of an unpolarized reference line [11].

The technique was originally applied to heliumlike Fe^{24+} [11]. The results of this measurement are shown in Fig. 7. Recently, we have applied the technique to a measurement of the polarization of the K-shell transitions in heliumlike Ti^{20+}. The titanium ions were excited about 100 eV above the direct electron-impact excitation threshold and simultaneously observed with a Si(111) crytal at $\theta = 24.7^o$ and a Si(220)

crytal at $\theta = 43.1^o$. The details of this measurement will be described elsewhere [18]. The results from this measurement are also given in Fig. 7. For comparison, the figure shows the polarization predictions for different heliumlike ions from relativistic distorted-wave calculations [11]. Very good agreement is found.

The figure also shows the measured value for line w in heliumlike Sc^{19+} measured by Henderson *et al.* [19]. This datum was obtained with a modified technique. Instead of using two crystals with different reflection properties, only one crystal was used but measurements were made in two planes of diffraction. The first was made in the same plane as described above; the second was made in the plane perpendicular to the first by rotating the entire spectrometer by 90°. The latter technique has also been applied to measurements of the linear polarization of $3s \rightarrow 2p$ transitions in neonlike Ba^{46+} [20].

In order to test the predictions away from threshold measurements are currently in progress at the Livermore high-energy EBIT facility to determine the linear polarization of the heliumlike Fe^{24+} lines at very high electron beam energy. These measurements employ two LiF crystals cut to the (220) and (200) planes. Results for the w line obtained at beam energies as high as 120 keV are shown in Fig. 8. The results are compared to predictions and good agreement is found. The analysis of the remaining heliumlike lines is still in progress and will be published at a future date [21].

5. Conclusion

Because an EBIT uses a monoenergetic electron beam, polarization effects are maximized. This provides a unique opportunity to test the calculations of the linear polarization of the line emission from highly charged ions in a controlled laboratory

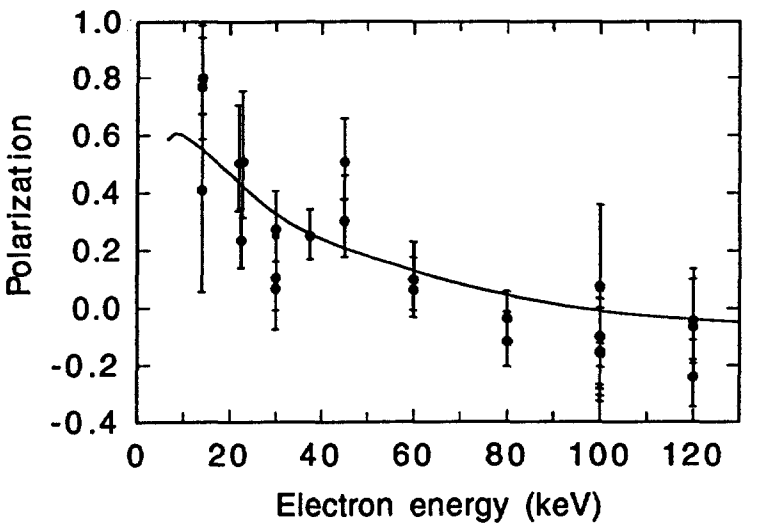

Figure 8: Measured polarization values of the resonance line w heliumlike Fe^{24+} for different electron beam energies from Ref. [21]. Predictions from Inal and Dubau from Ref. [12] are shown for comparison.

setting.

Depsite this great opportunity only a small number of such measurements have been performed to date. These include measurements of the 1–2 K-shell line emission from heliumlike Sc^{19+} [19] and Fe^{24+} [11] mentioned above, and measurements of the $3s \rightarrow 2p$ line emission in neonlike Ba^{46+} [20]. These measurements were performed at or close to threshold for electron-impact excitation. As we have shown, new measurements have been undertaken at the Livermore EBITs to extend the polarization measurements to the K-shell transitions of Ti^{20+} and to electron energies nearly twenty times above threshold in the case of Fe^{24+}. So far, very good agreement with relativistic distorted-wave calculations was found [12,22,23].

Polarization measurements with the Livermore EBIT have recently also been ex-

tended to cover dielectronic satellite emission of lithiumlike, berylliumlike, and boron-like iron [24,25], as discussed by Shlyaptseva *et al.* in these proceedings. These measurements test the accuracy of the calculations of alignment in resonant processes. Again, good agreement was found.

In addition, polarization measurements also have been concerned with L-shell transitions of Fe^{23+}, as discussed by Savin, Gu, and Beiersdorfer in these proceedings. These measurements were made at rather low beam energies ($\approx$ 2000 eV). At such low electron energies, the EBIT source no longer represents an ideal beam-ion collision experiment. The thermal electron motion perpendicular to the beam direction starts to play an important role and depolarization effects become relevant. However, as the contribution by Savin *et al.* shows, such depolarization effects are small compared to the accuracy limits of a given polarization measurement and to first approximation can be ignored or approximately accounted for. However, as the electron energy is yet smaller ($<$ 1000 eV), such effects may play a significant role.

Measurements of polarization are still only in their infancy and many classes of measurements have yet to be performed. For example, no measurements that include substantial cascade contributions have yet been made and compared with theory. The presence of a nuclear magnetic field was shown to have a strong effect on the observed linear polarization in heliumlike Sc^{19+} [19]. But this has not been investigated in any other system. Aluminum would be a suitable candidate, since this element has been employed routinely in investigations of laser-produced plasmas.

Because of the growing importance of plasma polarization spectroscopy in the research of high-temperature plasmas, we expect that many more measurements of the linear polarization of x-ray lines (and of UV, and visible lines) will be undertaken with EBITs. Because only very little has been studied so far, the field represents a fertile ground for exciting new discoveries and the development of novel, polarization-

based spectral diagnostics.

Acknowledgments

The author would like to G. Brown, V. Decaux, J. Lepson, S. Utter, and K. Widmann for their contributions to the measurements and analyses presented. This work was supported by the Department of Energy, Office of Basic Energy Science, Division of Chemical Science, and the National Aeronautics and Space Administration X-Ray Astronomy Research and Analysis Program under work order W-19127 and performed under the auspices of the Department of Energy by Lawrence Livermore National Laboratory under contract W-7405-ENG-48.

References

[1] S. Chantrenne, P. Beiersdorfer, R. Cauble, and M. B. Schneider, Phys. Rev. Lett. **69**, 265 (1992).

[2] K. L. Wong, P. Beiersdorfer, K. J. Reed, and D. A. Vogel, Phys. Rev. A **51**, 1214 (1995).

[3] P. Beiersdorfer, T. W. Phillips, K. L. Wong, R. E. Marrs, and D. A. Vogel, Phys. Rev. A **46**, 3812 (1992).

[4] P. Beiersdorfer, M. B. Schneider, M. Bitter, and S. von Goeler, Rev. Sci. Instrum. **63**, 5029 (1992).

[5] A. J. Smith, P. Beiersdorfer, V. Decaux, K. Widmann, K. J. Reed, and M. H. Chen, Phys. Rev. A **54**, 462 (1996).

[6] K. Wong, P. Beiersdorfer, M. H. Chen, R. E. Marrs, K. J. Reed, J. H. Scofield, D. A. Vogel, and R. Zasadzinski, Phys. Rev. A **48**, 2850 (1993).

[7] P. Beiersdorfer, A. L. Osterheld, M. H. Chen, J. R. Henderson, D. A. Knapp, M. A. Levine, R. E. Marrs, K. J. Reed, M. B. Schneider, and D. A. Vogel, Phys. Rev. Lett. **65**, 1995 (1990).

[8] J. R. Oppenheimer, Z. Phys. **43**, 27 (1927).

[9] I. C. Percival and M. J. Seaton, Philos. Trans. R. Soc. London **A251**, 113 (1958).

[10] R. M. Steffen and K. Alder, in *The Electromagnetic Interaction in Nuclear Spectroscopy*, edited by W. D. Hamilton (North-Holland, New York, 1975), p. 505.

[11] P. Beiersdorfer, D. A. Vogel, K. J. Reed, V. Decaux, J. H. Scofield, K. Widmann, G. Hölzer, E. Förster, O. Wehrhan, D. W. Savin, and L. Schweikhard, Phys. Rev. A **53**, 3974 (1996).

[12] M. K. Inal and J. Dubau, J. Phys. B **20**, 4221 (1987).

[13] M. K. Inal and J. Dubau, J. Phys. B **22**, 3329 (1989).

[14] A. H. Gabriel, Mon. Not. R. Astron. Soc. **160**, 99 (1972).

[15] A. Burek, Space Sci. Instrum. **2**, 53 (1976).

[16] B. L. Henke, E. M. Gullikson, and J. C. Davis, At. Data Nucl. Data Tables **54**, 181 (1993).

[17] P. Beiersdorfer, J. Crespo López-Urrutia, V. Decaux, K. Widmann, and P. Neill, Rev. Sci. Instrum. **68**, 1073 (1997).

[18] P. Beiersdorfer, G. V. Brown, S. B. Utter, E. J. Clothiaux, and A. J. Smith, in preparation .

[19] J. R. Henderson, P. Beiersdorfer, C. L. Bennett, S. Chantrenne, D. A. Knapp, R. E. Marrs, M. B. Schneider, K. L. Wong, G. A. Doschek, J. F. Seely, C. M. Brown, R. E. LaVilla, J. Dubau, and M. A. Levine, Phys. Rev. Lett. **65**, 705 (1990).

[20] E. Takács, E. S. Meyer, J. D. Gillaspy, J. R. Roberts, C. T. Chandler, L. T. Hudson, R. D. Deslattes, C. M. Brown, J. M. Laming, J. Dubau, and M. K. Inal, Phys. Rev. A **54**, 1342 (1996).

[21] P. Beiersdorfer, J. K. Lepson, and K. Widmann, in preparation .

[22] H. L. Zhang, D. H. Sampson, and R. E. H. Clark, Phys. Rev. A **41**, 198 (1990).

[23] K. J. Reed and M. H. Chen, Phys. Rev. A **48**, 3644 (1993).

[24] A. S. Shlyaptseva, R. C. Mancini, P. Neill, and P. Beiersdorfer, Rev. Sci. Instrum. **68**, 1095 (1997).

[25] A. S. Shlyaptseva, R. C. Mancini, P. Neill, P. Beiersdorfer, J. Crespo López-Urrutia, and K. Widmann, Phys. Rev. A **57**, 888 (1998).